Review Article
pISSN 1738-2637 / eISSN 2288-2928
J Korean Soc Radiol 2013;69(1):11-22
http://dx.doi.org/10.3348/jksr.2013.69.1.11

대한영상의학회지

The Role and Utility of Diffusion-Weighted Imaging in Assessment of Head and Neck Tumors: A Review Article[1]

두경부 종양의 평가에 있어서 확산강조영상의 역할과 유용성: 종설[1]

Yu Li Sol, MD[1], Hak Jin Kim, MD[1], Byung Joo Lee, MD[2]

Departments of [1]Radiology, [2]Otolaryngology, Biomedical Research Institute, Pusan National University Hospital, Pusan National University School of Medicine, Busan, Korea

Conventional MRI and CT are the chosen imaging modalities when evaluating head and neck cancers; however, sometimes both diagnostic tools yield low sensitivity and accuracy in making the diagnosis, staging, and assessing the post-treatment response. This article reviews the role and utility of diffusion-weighted imaging (DWI) in assessing head and neck cancer. DWI is a technique which analyzes the structures of biologic tissues at a microscopic level. Apparent diffusion coefficient value, determined from DWI, can help detect the differences in the microstructures of tumor tissues and non-tumor tissues. Therefore, DWI is a useful technique in a clinical practice, which provides information of histopathological characterization, differential diagnosis, and stage of head and neck cancer and assessment of treatment response.

Index terms
Head and Neck Tumors
MRI
Diffusion-Weighted Imaging
Apparent Diffusion Coefficient Value

Received March 5, 2013; **Accepted** May 3, 2013
Corresponding author: Hak Jin Kim, MD
Department of Radiology, Biomedical Research Institute, Pusan National University Hospital, Pusan National University School of Medicine, 179 Gudeok-ro, Seo-gu, Busan 602-739, Korea.
Tel. 82-51-240-7371 Fax. 82-51-244-7534
E-mail: hakjink@pusan.ac.kr

This study was supported by a 2-year Research Grant of Pusan National University.

INTRODUCTION

CT and magnetic resonance imaging (MRI) are the two selected imaging modalities for the diagnosis and staging of head and neck tumors. Although both diagnostic tools have high accuracies for detecting and staging such cancers, the imaging features of benign and malignant head and neck lesions are often non-specific and overlapping, because these techniques evaluate the macroscopic morphologies of biologic tissues and do not reflect microstructural differences (1). Although both diagnostic tools have high accuracies for detecting and staging such cancers.

However, advanced MR techniques are being developed which provides information concerning the metabolic, molecular and pathophysiological aspects of tumors; and imaging biomarkers are important tools for the detection and characterization of cancers and for monitoring the response to therapy.

Diffusion-weighted imaging (DWI) is a non-invasive technique that analyzes the structures of biologic tissues at the microscopic level. Furthermore, DWI has the advantages of being non-invasive, thus, requiring no exogenous contract agents or ionizing radiation, it owns a short imaging time and can be easily incorporated into routine evaluations (2, 3).

Several studies (4-7) have suggested that DWI could be used to differentiate and characterize head and neck lesions and to monitor responses to therapy. Recently, DWI has been used clinically to differentiate benign and malignant head and neck lesions. In this paper, we review the role and utility of DWI for assessing head and neck tumors and discuss the limitations and future perspectives.

THE BIOLOGICAL CONCEPT OF DWI IN HEAD AND NECK TUMORS

Biological tissues are composed of intra- and extra-cellular com-

partments. In these tissues, water molecules are in a state of continuous exchange between these two compartments. In the human body, free diffusion of water molecules does not exist due to restrictions imposed by cell membranes and molecular boundaries.

The biophysical mechanism underlying DWI is based on the different microscopic mobilities of water molecules in biological tissues. This mobility or Brownian motion, is highly influenced by the cellular environment, and is restricted by cellular packing and barriers, such as, intracellular organelles, cell membranes, and macromolecules.

Diffusion in the extracellular space is restricted by macromolecules and membranous organelles, whereas diffusion in the intracellular space is more restricted by physical (macromolecules and organelles) and chemical (specific binding and protein transitions and movements) factors and syneresis. Diffusion-weighted MR images are obtained using an echo planar imaging (EPI) technique, which can be performed rapidly and enables data acquisition, with different b-values, within a relatively short amount of time (8).

During diffusion-weighted MRI, translational motion causes phase dispersion of excited water protons, which leads to a DWI signal loss (9, 10) that can be quantified by calculating the apparent diffusion coefficients (ADC). ADCs are calculated during post-processing using at least two different b-values. Variations in ADC values reflect redistributions of water molecules between intracellular and extracellular tissue compartments, and thus, ADC values depend on microstructure and pathophysiologic state (4, 11).

UTILITY OF DWI IN HEAD AND NECK TUMORS

Characterization and Differential Diagnosis of Head and Neck Tumors

The differential diagnosis of benign and malignant lesions of the head and neck is critical as it enables clinicians to adopt appropriate management strategies. DWI has the ability to differentiate malignant and benign tumors in the head and neck lesions.

Mechanism of Diffusion Restriction in Malignant Tumors

The reason why malignant tumors have lower ADC values is poorly understood. However, the concept of restricted diffusivity in malignant tumors can be explained as follows. Within malignant tumors, the translational motion of water molecules is diminished due to increased extracellular space tortuosity, increased nuclear-to-cytoplasmic ratio, hyperchromatism, and hypercellularity. These histopathological characteristics of malignant tumor reduce the extracellular to intracellular volume ratio and the diffusion space available to water molecules, which reduce ADC values (4, 6).

The ADC Values for Benign and Malignant Lesions

The mean ADC values for differentiation of benign and malignant lesions in the head and neck have been reported as patterns of disease entity or lesion sites. The mean ADC values for differentiation of benign and malignant lesions in the head and neck were revealed with a wide range. In general, cut-off values for differential diagnosis of benign and malignant lesions have been accepted as under 0.9 - 1.1 $\times 10^{-3}$ mm^2/s (Figs. 1, 2). Kwon et al. (12) reported sensitivity, specificity, positive predictive, negative predictive values and accuracy as 92%, 66.6%, 87.8%, 76.1% and 85%, respectively, in differentiation of benign and malignant lesions in the pharynx with the cut-off ADC value as 1.1 $\times 10^{-3}$ mm^2/s. Sasaki et al. (13) found that the ADCs of malignant tumors ($0.87 \pm 0.32 \times 10^{-3}$ mm^2/s) were significantly lower than those of benign ($1.35 \pm 0.29 \times 10^{-3}$ mm^2/s, $p < 0.0001$) and inflammatory ($1.50 \pm 0.50 \times 10^{-3}$ mm^2/s, $p < 0.0002$) lesions. Friedrich et al. (14) reported lower mean ADC value for head and neck squamous cell carcinoma (SCC) of $0.64 \pm 0.28 \times 10^{-3}$ mm^2/s, and the result was probably because of one specific disease entity of squamous cell carcinoma enrolled in the study.

In the parotid gland, however, due to an overlap not only within the group of benign and malignant lesions but also an overlap between these groups, diagnoses should not be addressed on the basis of ADC values solely (15). Especially among those parotid gland tumors, Warthin's tumors revealed lower ADC values (mean ADC value of $0.89 \pm 0.16 \times 10^{-3}$ mm^2/s) than those of pleomorphic adenoma and carcinoma (Fig. 3). This low ADC value is related to the hypercellularity of Warthin's tumor (16).

1.5 T versus 3.0 T

The majority of the previous studies have been performed using 1.5 telsa (T) magnetic resonance systems. Srinivasan et al. (6) reported ADC values for benign and malignant head and

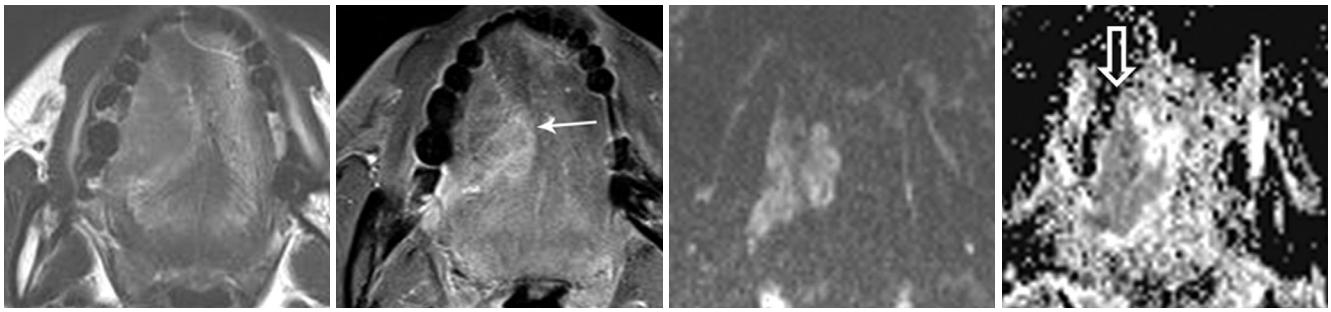

A B C D

Fig. 1. A 47-year-old woman with SCC in the tongue. Axial T2- **(A)** and contrast enhanced T1-weighted images **(B)** show a mass in the right lateral tongue (arrow). DWI with b value of 1000 **(C)** reveals high signal intensity of the mass. The mean ADC value within the lesion measured 0.914×10^{-3} mm^2/s on the ADC map image (**D,** open arrow).
Note.—ADC = apparent diffusion coefficient, DWI = diffusion-weighted imaging, SCC = squamous cell carcinoma

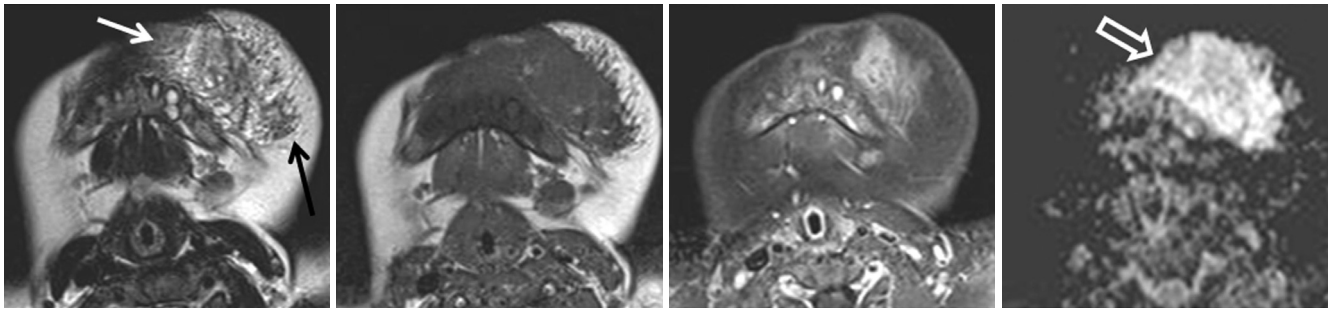

A B C D

Fig. 2. A 5-year-old male with lymphangioma in the left cheek. Axial T2- **(A)**, T1-weighted images **(B)** reveal a mass with heterogenous signal intensity (arrows). The mass is enhanced in the central portion on contrast enhanced T1-weighted image **(C)**. The mean ADC value of the mass measured 1.936×10^{-3} mm^2/s on the ADC map image (**D,** open arrow).
Note.—ADC = apparent diffusion coefficient

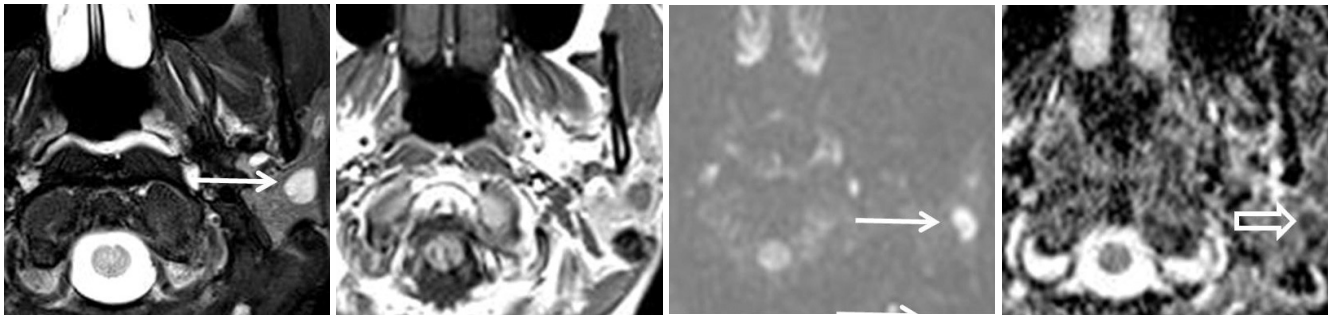

A B C D

Fig. 3. A 47-year-old female with Warthin's tumor in the left parotid gland. Axial T2-weighted image **(A)** shows a round bright signal intensity mass (arrow). On T1-weighted image **(B)** the mass reveals low signal intensity. The mass represents high signal intensity on the DWI (**C,** arrow) and the ADC map image (**D,** open arrow). The ADC value of the lesion measured 0.731×10^{-3} mm^2/s.
Note.—ADC = apparent diffusion coefficient, DWI = diffusion-weighted imaging

neck lesions at 3.0 T, and found a significant difference ($p < 0.004$) between the mean ADC values of benign ($1.50 \pm 0.48 \times 10^{-3}$ mm^2/s) and malignant ($1.07 \pm 0.29 \times 10^{-3}$ mm^2/s) lesions. However, it is unclear as to how ADC values vary at different field strengths, although the results obtained by Srinivasan et al. (6) were similar to those obtained using 1.5 T MR systems.

Lymphoma versus Carcinoma

Some investigators have also reported significantly lower ADC values in lymphoma than in SCC of the head and neck (Fig. 4). Maeda et al. (7) reported a mean ADC value of $0.96 \pm 0.11 \times 10^{-3}$ mm^2/s for SCC and of $0.65 \pm 0.09 \times 10^{-3}$ mm^2/s for lymphoma ($p < 0.001$). In a study by Sumi et al. (17), authors evaluated the di-

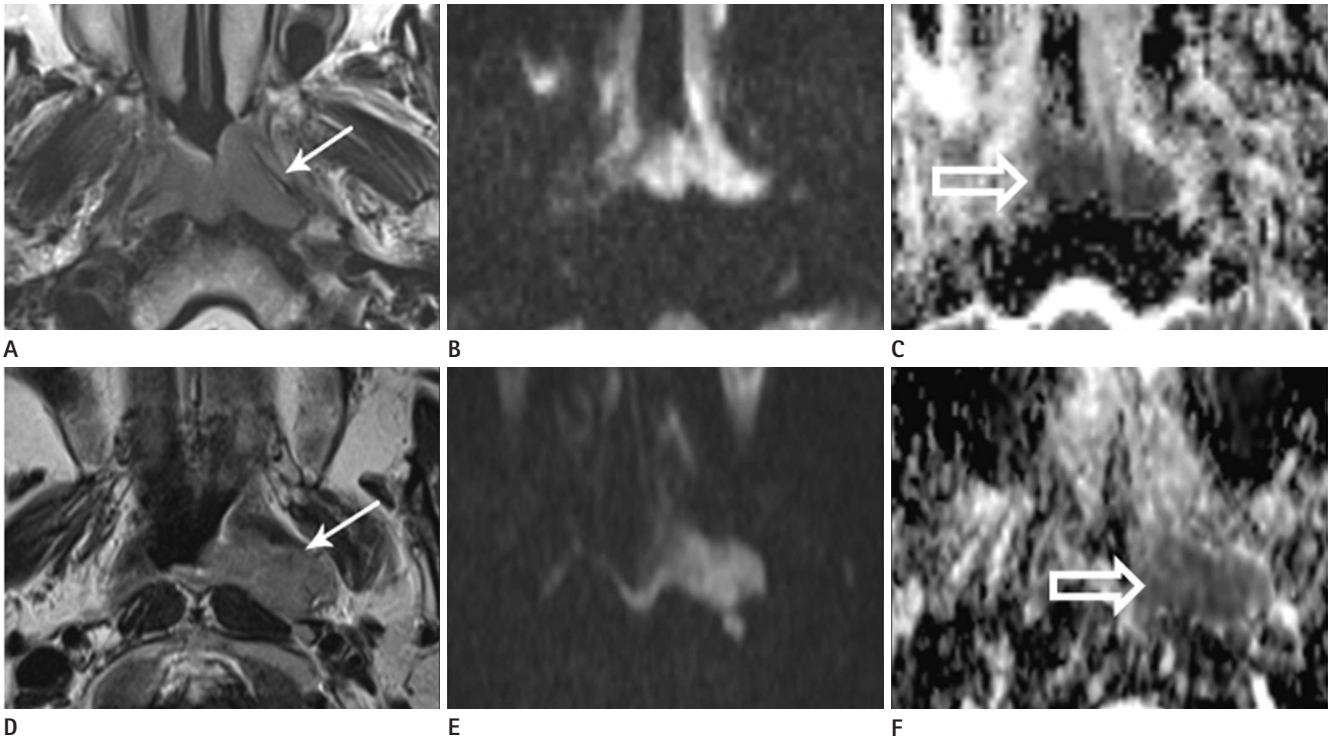

Fig. 4. MR images of diffuse large B-cell lymphoma **(A–C)** in a 71-year-old woman and SCC **(D–F)** in a 58-year-old woman. In both patients, masses are located in the left nasopharynx (arrow), revealing hypointensity on T2-weighted image **(A, D)** and hyperintensity on DWI **(B, E)**. The ADC value measured 0.526 × 10^{-3} mm^2/s in lymphoma (**C,** open arrow), which was lower than that of patient with SCC (**F,** 0.877 × 10^{-3} mm^2/s, open arrow).
Note.—ADC = apparent diffusion coefficient, DWI = diffusion-weighted imaging, SCC = squamous cell carcinoma

agnostic ability of DWI with respect to the differentiation of lymphomas and carcinomas in the pharynx, and found that the ADCs of lymphomas (0.454 ± 0.075 × 10^{-3} mm^2/s) were significantly lower than those of pharyngeal carcinomas (0.863 ± 0.238 × 10^{-3} mm^2/s). Furthermore, when an ADC < 0.560 × 10^{-3} mm^2/s was used to predict lymphoma, accuracy was maximal at 96% whereas sensitivity, specificity, positive predictive value, and negative predictive value were 100, 94, 86, and 100%, respectively. The lower ADC values of lymphoma than SCC can be explained by the histopathological characteristics of lymphomas, which contained densely packed cells with relatively high nuclear-to-cytoplasm ratios that decreased water diffusivity in the intra- and extracellular spaces.

Evaluation of Pathological Lymph Nodes

It is difficult to differentiate inflammatory lymph nodes (LNs) from metastatic lymphadenopathy on CT or MR images. Furthermore, morphologic features of malignancy, such as, necrosis, indistinct margins, and loss of fatty hilum in lymph nodes, are relatively infrequent findings, especially for small (< 10 mm) metastatic lymph nodes (18). Thus, anatomic imaging modalities, such as, CT and MR imaging rely mainly on node sizes to detect malignant and metastatic lymphadenopathies because of a lack of reliable morphologic criteria (19). In particular, for conventional MRI, the morphologic criteria used for nodal staging do not seem to exceed those of CT. As a metabolic imaging, ^{18}F-fluorodeoxyglucose-positron emission tomography (FDG-PET) scans help this differentiation, but they cannot detect small tumor deposits with non-enlarged LNs. They are also expensive with less availability and have low spatial resolutions (20).

Several studies have reported that DWI can differentiate malignant and benign lymph nodes in the neck, and that malignant nodes exhibit lower ADC values than benign lymph nodes (5, 20, 21). In a study that evaluates the use of DWI for the detection of nodal metastasis in head and neck SCC, Vandecaveye et al. (21) reported that the mean ADC of malignant LNs (0.85 ± 0.27 × 10^{-3} mm^2/s) was significantly lower than that of benign LNs (1.19 ± 0.22 × 10^{-3} mm^2/s), and at a threshold ADC of 0.94 × 10^{-3} mm^2/s, obtained a sensitivity of 84%, a specificity of 94%, and an accuracy of 91% for the differentiation of malignant and

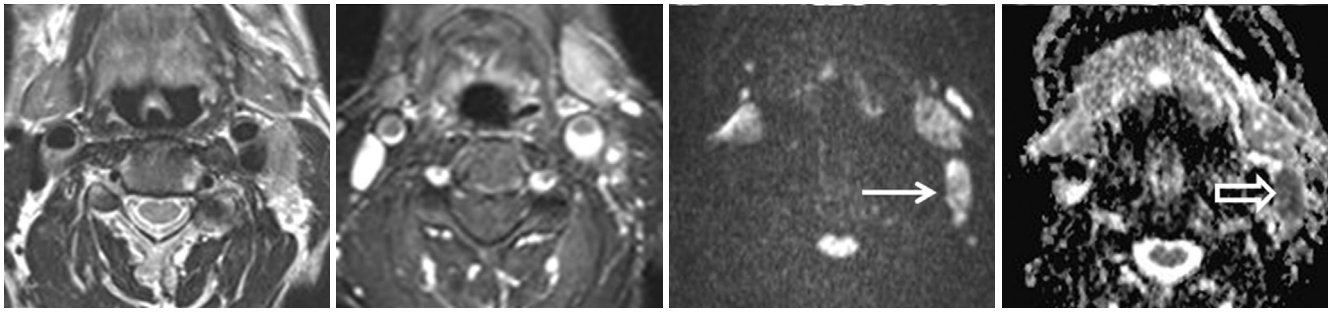

Fig. 5. A 64-year-old man with lymph nodal metastasis. Axial T2-weighted **(A)** and contrast enhanced T1-weighted images **(B)** reveal a 1-cm sized lymph node at the left level II, which is difficult to differentiate benign and malignant node. However, the node shows hyperintensity on DWI (**C,** arrow) and decreased ADC value (0.654×10^{-3} mm^2/s) on the ADC map image (**D,** open arrow).
Note.—ADC = apparent diffusion coefficient, DWI = diffusion-weighted imaging

benign LNs.

DWI is especially helpful for diagnosis of small malignant lymph nodes which is difficult with conventional CT or MR images (Fig. 5). Small lymph nodes with a maximum short axial diameter below 10 mm are more challenging for differential diagnosis, because the mere use of this size criterion will result in misclassification of malignant lymph nodes as normal on MRI evaluation. de Bondt et al. (22) studied the ADC value in especially small lymph nodes (smaller than 10 mm) in the head and neck squamous cell carcinoma, and reported that sensitivity 92.3% and specificity 83.9% with the ADC threshold as 1.0×10^{-3} mm^2/s. Within this study, observations on the predominantly small lymph nodes show that the ADC criterion is the strongest independent predictor of presence of metastasis.

King et al. (23) reported that DWI showed significant differences between malignant nodes of SCC, lymphoma, and nasopharyngeal carcinoma (NPC), and found that ADC threshold values could help differentiate SCC and lymphoma (23). Mean ADC values for nodes of lymphoma, NPC, and SCC were $0.664 \pm 0.071 \times 10^{-3}$ mm^2/s, $0.802 \pm 0.128 \times 10^{-3}$ mm^2/s, and $1.057 \pm 0.169 \times 10^{-3}$ mm^2/s, respectively, with significant differences between SCC and lymphoma or NPC ($p < 0.001$) and between NPC and lymphoma ($p < 0.04$).

DWI has also been used to characterize enlarged necrotic nodes associated with inflammation or neoplastic diseases, especially when the differentiation of central necrosis in metastatic nodes and in infectious necrotic nodes is difficult by conventional MRI. Koç et al. (24) reported that abscesses and necrotic lymphadenitis appear hyperintense on DW images and exhibit lower ADC values than necrotic nodal metastases that appear hypo-intense on DW images and have higher ADC values.

The difference between the ADC values of benign and malignant lymph nodes is probably related to different cellularities and histopathological features. As mentioned, malignant nodes have enlarged nuclei exhibits hypercellularity, and hyperchromatism, which decreases the ADC values of malignant lymph nodes.

Nevertheless, ADC values have potential for the detection of sub-centimeter nodal metastases, the lower in-plane resolution of ADC maps and potential image artifacts, especially if the nodes are located at the air-tissue interface, thus, result in technical limitations. Partial volume effects from the regions of interest which are used to measure the ADC values of these small lymph nodes may also lead to inaccurate ADC values.

Differentiation of Viable Tissue and Necrosis in Malignant Tumors

For head and neck cancer patients, an accurate depiction of viable and necrotic tumor regions is important for diagnosis and treatment planning, as well as being essential when choosing a biopsy site, because unsuitable choices may result in incorrect histological diagnosis. On contrast-enhanced T1-weighted images, tumors are usually visualized as contrast-enhancing lesions, and biopsy usually reveals that the enhanced portions of tumors contain viable tumor cells. However, non-enhanced portions may contain viable or necrotic tissues.

Razek et al. (25) investigated whether DWI could differentiate viable and necrotic regions in head and neck tumors. In this study, the mean ADC of viable tumor portions was $1.17 \pm 0.33 \times 10^{-3}$ mm^2/s and that of necrotic portions was $2.11 \pm 0.05 \times 10^{-3}$ mm^2/s. Low-signal-intensity regions with low ADC values on the

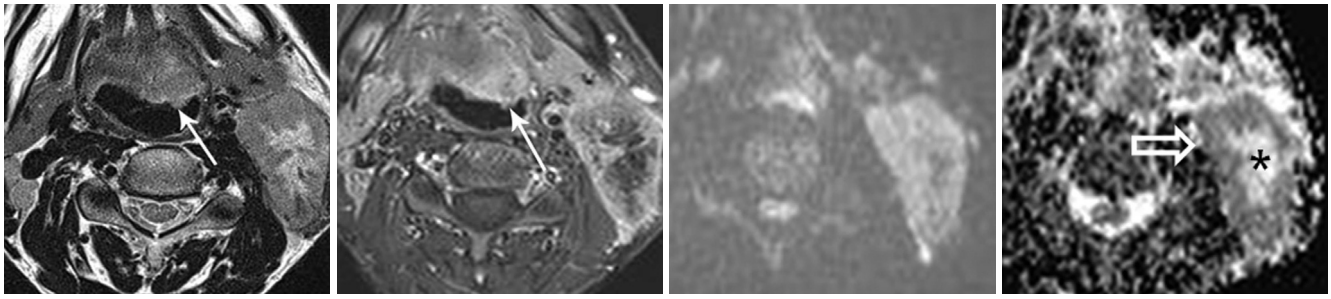

Fig. 6. A 49-year-old man with squamous cell cancer in the left tongue. Axial T2-weighted **(A)** and contrast enhanced T1-weighted images **(B)** show a malignant mass in the left tongue base (arrow), biopsy-proven SCC. A large metastatic lymphadenopathy is also seen in the left level II. The node shows hyperintensity with central hypointensity on DWI **(C)**. The ADC map **(D)** reveals low signal intensity of the enhanced peripheral part of the tumor with low ADC value (0.987×10^{-3} mm^2/s, open arrow) representing a viable portion of the tumor. The non-enhancing central part of the tumor shows high signal intensity with high ADC value (1.597×10^{-3} mm^2/s, asterisk) representing a necrotic portion of the tumor.
Note.—ADC = apparent diffusion coefficient, SCC = squamous cell carcinoma

ADC maps were found to represent viable tumor regions, whereas high signal intensities with high ADC values represented necrotic regions, and these ADC values of viable tumors was reported to be significantly lower than that for necrotic parts (Fig. 6). The sensitivity, specificity, and accuracy of ADC values were 92.9%, 93%, and 94.6%, respectively.

Tumor necrosis is characterized by increased membrane permeability and cell membrane breakdowns, which results in free diffusion and an increase in the mean free-path length of diffusing molecules. These changes lead to increased mobility and water molecule diffusion in necrotic regions (25).

The Differentiation of Tumor Recurrence and Post-Treatment Change

Currently, majority of patients with head and neck cancer undergo induction chemotherapy, and concurrent chemo-radiotherapy (CCRT) with surgery. After surgery, normal anatomic structures can be extensively distorted, and such radiotherapy can cause edema, fibrous inflammatory reactions, and scarring of adjacent normal soft tissues. The challenge presented to imaging methods is the differentiation of tumor recurrences and post-treatment changes, which is important for clinical decision-makings and patient management. However, after surgery and CCRT in patients with head and neck cancer, residual and recurrent lesions and treatment-induced changes exhibit similar imaging characteristics, and are, therefore, difficult to differentiate on routine follow-up MR images (26). Although FDG-PET/CT can aid the detection of recurrent head and neck cancer, it is prone to false positives owing to inflammatory changes within the first 4 months after radiation therapy (27). In addition, PET commonly produces false positive findings and suffers from low spatial resolutions that cause false negative findings within small volume of diseases. Biopsy is often necessary, but results of histopathologic speciments can be inaccurate due to sampling errors. Surgeons also fear initiating or aggravating radiation necrosis in previously irradiated areas when multiple or deep biopsy specimens are obtained (28-30).

The results of recent studies deduce that diffusion-weighted MRI has the potential to distinguish post-radiation changes from recurrent cancer based on the ADC value differences (Fig. 7). Abdel Razek et al. (31) reported significant mean ADC value differences between post-treatment changes and residual/recurrent head and neck cancer; the mean ADC value of residual or recurrent lesions ($1.17 \pm 0.33 \times 10^{-3}$ mm^2/s) was significantly lower ($p < 0.001$) than that of post-treatment changes ($2.07 \pm 0.25 \times 10^{-3}$ mm^2/s).

Differences in ADC values reflect distinct histopathologic differences, water proton distribution in tumors, and post-treatment soft tissue changes. In tissues exhibiting post-treatment change, histopathological characteristics, such as, low cellularity associated with variable degrees of edema and inflammatory reaction increasing interstitial water contents, and thus, increases the ADC values (4, 31, 32).

Assessment of Treatment Response

As a reliable prediction method of therapeutic response during the early treatment stage, imaging markers may assist in the tailoring of treatment regimens and improve overall clinical out-

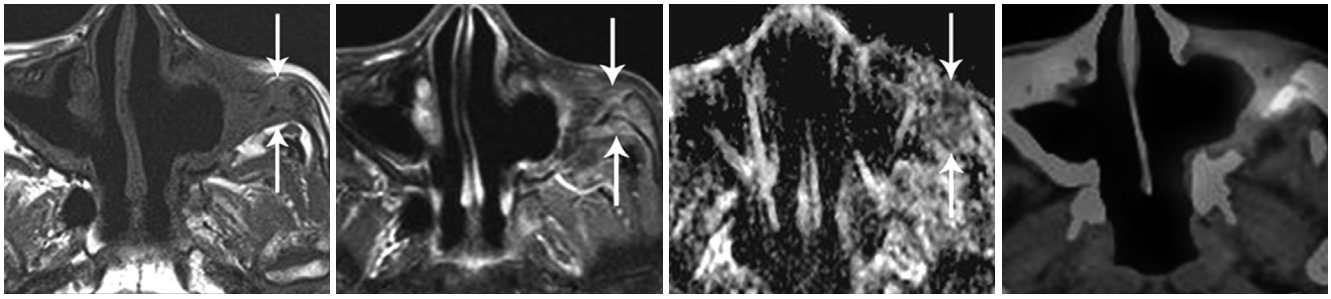

A B C D

Fig. 7. A 71-year-old man with recurrent squamous cell cancer in the left maxillary sinus. Axial T1-weighted image **(A)** shows a mass at the lateral margin of previous resection site in the left maxillary sinus (arrows). On axial contrast T1-weighted image **(B)**, the lesion is well-enhanced. The ADC map image **(C)** shows low signal intensity with a mean value of 0.581 x 10^{-3}mm^2/s, representing recurrence. Increased FDG uptake is noted in the lesion on PET/CT scan **(D)**.
Note.—ADC = apparent diffusion coefficient, FDG = fluorodeoxyglucose, PET/CT = positron emission tomography/CT

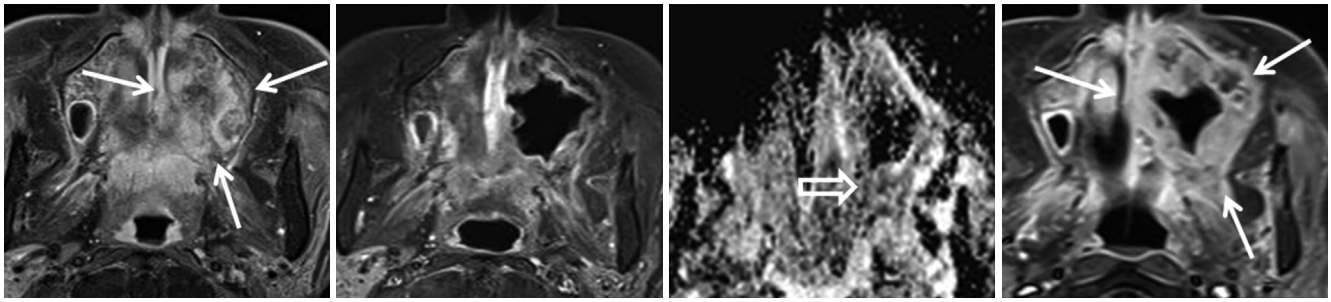

A B C D

Fig. 8. A 54-year-old man with adenoid cystic carcinoma in the left hard palate. Initial contrast enhanced T1-weighted image **(A)** reveals an enhancing solid mass in the left palatal bone (arrows). Follow-up T1-weighted image **(B)** after post-radiation 1 1/2 year **(B)** shows markedly interval improving state. However, on the ADC map image at the same day **(C)**, a focal area reveals diffusion restriction with a mean value of 0.74 × 10^{-3} mm^2/s (open arrow), representing a remnant mass. The lesion is aggravated diffusely on the 5-month follow-up contrast enhanced T1-weighted image (**D,** arrows).
Note.—ADC = apparent diffusion coefficient

comes. Several studies have already been published on the roles of DWI in the assessment and prediction of treatment responses for animal models and human brain tumors. Previous studies of animal models (33-36) and of human brain tumors (37-40) have demonstrated the sensitivity of DWI for detecting early changes induced by chemotherapy. In a study by Zhao et al. (41), it was found that ADC increased in a mouse RIF-1 tumor after treatment with the anticancer drug cyclophosphamide prior to a reduction in tumor volume, and thereafter, several groups have shown increased water diffusions through experimental tumors after treatment with anti-cancer drugs (35, 39) or gene therapy (36, 42). Furthermore, clinical studies on the efficacy of ADC for the prediction or early detection of treatment response have been conducted on brain tumors (43), breast cancer (44), and cervical cancer (45).

These several studies in animal and human models have shown that ADC values increase after treatment with antitumor therapies prior to reductions in tumor volume, and thus, enable the early detections of tumor response. Furthermore, in these studies it was also found that tumors with higher ADC values were associated with a reduced response to therapy, and low ADC tumors responded better to treatments than high ADC tumors.

In the follow-up imaging work-up of head and neck malignant lesions, the assessment of treatment response is often difficult for conventional CT or MR imaging due to anatomical derangement or alteration of primary lesions (Fig. 8). Recently, the potential use of ADC values for the prediction or early detection of treatment response in head and neck cancer was described by Kim et al. (46). In this study, patients that responded favorably to chemoradiation therapy were found to have significantly lower pretreatment ADC values than partial respondents or non-respondents. Furthermore, a significant increase in ADC was observed in full respondents within 1 week of treatment, and

complete respondents also showed significantly greater increases in ADC values than partial respondents after one week of chemoradiation therapy.

A change in ADC values has also been reported to be associated with increased numbers of apoptotic cells and loss of cellularity during apoptosis targeted cancer therapy (47). Although the mechanism underlying increased water diffusions following cytotoxic chemotherapy in experimental and human tumors is not fully understood, the cytotoxic chemotherapy triggers apoptotic pathways which reduce cell density and enlarge extracellular spaces, which could explain the increase in ADC values observed after treatment (48). Although the mechanism underlying increased water diffusions following cytotoxic chemotherapy in experimental and human tumors is not fully understood, the cytotoxic chemotherapy which triggers apoptotic pathways reducing cell density and enlarging extracellular spaces are explanations for the ADC value increases after the treatment.

In addition, several studies have been conducted to determine the merits of imaging modalities, such as, perfusion CT (49), arterial spin labeling (50), and blood oxygen level dependent MRI (51), for the predictions of therapeutic responses. Zima et al. (52) reported that higher levels of blood flow and blood volume as measured by CT perfusion may be correlated with better oxygen and drug delivery, and suggested that such techniques might be useful to predict responses to radiotherapy and/or chemotherapy. In these studies, the authors emphasized the role that the tumor vasculature plays in the supply of nutrients and oxygen and acting as the chemotherapeutic agents to tumor cells.

TECHNICAL PITFALLS OF DWI

Image quality in diffusion-weighted MRI is characterized by signal-to-noise ratio (SNR) and freedom from artifacts. To obtain high quality images for qualitative or quantitative assessments, scanning factors should be optimized to maximize SNR and reduce artifacts. In order to optimize SNR, parallel imaging should be used because this shortens echo-train lengths and reduces susceptibility artifacts, and the echo time (TE) should be as short as possible.

EPI pulse sequences are highly susceptible to magnetic field heterogeneities, which result in geometric distortion artifacts. The intrinsic difficulties associated with EPI, such as susceptibility artifacts, chemical shift artifacts, and Nyquist (N/2) ghosting artifacts in the phase-encoding direction, are considerably more severe in the head and neck regions. Susceptibility artifacts are caused by the many air-bone and soft tissue-bone interfaces in the head and neck region, and result in image distortions and can present serious problems during diffusion-weighted image analysis. Other sources of susceptibility artifacts include metallic dental fillings.

One way to reduce susceptibility artifacts is to acquire DWI using the sensitivity encoding (SENSE) technique. Reduced echo train length at SENSE DWI reduces susceptibility artifacts, and thus, provides images of higher overall quality (53, 54). Newer techniques, such as, split acquisition of fast spin-echo signals (SPLICE) (55), DWI with line scan data acquisition (LSDWI) (7), and fast asymmetric SE (56) which are insensitive to susceptibility artifacts, have also been recently proposed for the acquisition of DWI data.

In LSDWI, multiple diffusion-weighted, spin-echo column excitations are used to obtain a two-dimensional image. This method is relatively insensitive to motion artifacts because the images are constructed column by column, and the acquisition time required for an individual column is approximately equal to the TE (7).

EPI often contains an aliased image or 'ghost' displaced by N/2 point from the main image along the phase-encode axis. The so-called 'Nyquist (N/2) artifact' describes a ghost image in half view of the phase-encoding direction. These artifacts are caused by zigzag data acquisition patterns in the EPI sequence, and can be reduced by using a calibrated scan, which is obtained at the beginning of the EPI sequence with the phase-encoding gradient being turned off (57).

Motion artifacts in head and neck area on DWI are associated with the continuous physiological motions associated with breathing and swallowing. Another source of motion artifacts by DWI is the pulsation of large arterial vessels. Thus, careful selection of the reference slice, avoiding vascular structures, is mandatory to obtain good diffusion-weighted image quality and reliable information about the diffusion capacity of the tumor under investigation (14). Increasing the speed of image acquisition, which is now possible with single-shot EPI, and the use of parallel imaging also provides possible means of reducing this artifact (3).

Partial volume effects from the regions of interest used to mea-

sure ADC values of small lesions or lymph nodes may also lead to ADC value inaccuracies. Furthermore, as ADC maps suffer from relatively poor resolutions, ADC values of lesions located at air-tissue interfaces may be questionable with respect to their specificities and reproducibilities. However, several factors enable the detection of small nodal metastases or small lesions by DWI, and the use of improved EPI technology, dedicated coils, and dedicated sequence optimization enable EPI-related artifacts to be maximally reduce at a relatively high spatial resolution (58).

FUTURE PERSPECTIVES

Diffusion-weighted MRI clearly differentiates itself from other imaging modalities because it is the only imaging modality that is able to depict water movements at the cellular level. However, although DWI is regarded as biologic imaging modality, the inherent shortcomings associated with EPI and the above-mentioned technical pitfalls can be problematic. Thus, better image quality by optimizing SNRs and new techniques that reduce artifacts would improve the accuracy, sensitivity, and specificity of DWI with respect to differentiating diagnosis of head and neck cancers, the evaluation of pathologic lymph nodes, the contrast of viable and necrotic lesions in malignant tumors, the variation of tumor recurrence and post-treatment changes, and the assessment of treatment response.

In patients with head and neck cancer, if DWI could detect treatment efficacy at an earlier stage after anticancer therapy commencements, the ineffective therapies could be stopped quickly. Specifically in cases of when the therapy concerned has severe adverse effects, is expensive, or when alternative approaches to treatments are available. Furthermore, pre- and post-treatment ADC values have the potential to become image markers for the prediction or detection of early treatment response in patients with head and neck cancer whom have received chemotherapy or radiation therapy. However, larger controlled studies are required to determine the sensitivity and specificity of DWI more accurately in order to predict treatment responses.

SUMMARY

The biophysical mechanism underlying DWI concerns the random translational motion of water molecules in biological tissues, and the diffusion in biologic systems is affected by water exchanging between intracellular and extracellular compartments and the tortuosity of extracellular spaces.

The ADC values of malignant tumors are significantly lower than those of benign lesions. The histopathological characteristics of malignant tumors, such as, an elevated nuclear/cytoplasm ratio, hyperchromatism, and hypercellularity, reduce the extracellular to intracellular volume ratio and the space available for water molecule diffusion. The delineations of viable and necrotic tumor regions are essential for identifying biopsy sites, diagnosis and treatment planning. The mean ADC values of viable tumors have been reported to be significantly lower than those of necrotic regions. On conventional MR images, residual or recurrent lesions and treatment-induced changes appear similarly and are often difficult to distinguish. However, residual and recurrent lesions have lower ADC values than post-treatment changes. DWI changes may provide a means of determining, at an early stage, likely treatment outcomes. For most malignant tumors, successful treatment is reflected by an increase in ADC values.

DWI is a useful clinical technique that provides information about histopathological characteristics, differential diagnosis, and stages of head and neck cancer and it also provides a means of assessing treatment responses. Due to the inherent drawbacks associated with EPI and the technical pitfalls of DWI, new acquisition methods are needed to improve image quality and reduce artifacts. Furthermore, larger-scale studies are required to ascertain whether DWI offers a robust and reproducible means of determining responses to anticancer therapies.

REFERENCES

1. Lell M, Baum U, Greess H, Nömayr A, Nkenke E, Koester M, et al. Head and neck tumors: imaging recurrent tumor and post-therapeutic changes with CT and MRI. *Eur J Radiol* 2000;33:239-247
2. Neil JJ. Diffusion imaging concepts for clinicians. *J Magn Reson Imaging* 2008;27:1-7
3. Malayeri AA, El Khouli RH, Zaheer A, Jacobs MA, Corona-Villalobos CP, Kamel IR, et al. Principles and applications of diffusion-weighted imaging in cancer detection, staging, and treatment follow-up. *Radiographics* 2011;31:1773-1791

4. Wang J, Takashima S, Takayama F, Kawakami S, Saito A, Matsushita T, et al. Head and neck lesions: characterization with diffusion-weighted echo-planar MR imaging. *Radiology* 2001;220:621-630
5. Sumi M, Sakihama N, Sumi T, Morikawa M, Uetani M, Kabasawa H, et al. Discrimination of metastatic cervical lymph nodes with diffusion-weighted MR imaging in patients with head and neck cancer. *AJNR Am J Neuroradiol* 2003; 24:1627-1634
6. Srinivasan A, Dvorak R, Perni K, Rohrer S, Mukherji SK. Differentiation of benign and malignant pathology in the head and neck using 3T apparent diffusion coefficient values: early experience. *AJNR Am J Neuroradiol* 2008;29: 40-44
7. Maeda M, Kato H, Sakuma H, Maier SE, Takeda K. Usefulness of the apparent diffusion coefficient in line scan diffusion-weighted imaging for distinguishing between squamous cell carcinomas and malignant lymphomas of the head and neck. *AJNR Am J Neuroradiol* 2005;26:1186-1192
8. Schaefer PW, Grant PE, Gonzalez RG. Diffusion-weighted MR imaging of the brain. *Radiology* 2000;217:331-345
9. Lang P, Johnston JO, Arenal-Romero F, Gooding CA. Advances in MR imaging of pediatric musculoskeletal neoplasms. *Magn Reson Imaging Clin N Am* 1998;6:579-604
10. Szafer A, Zhong J, Gore JC. Theoretical model for water diffusion in tissues. *Magn Reson Med* 1995;33:697-712
11. Le Bihan D, Breton E, Lallemand D, Aubin ML, Vignaud J, Laval-Jeantet M. Separation of diffusion and perfusion in intravoxel incoherent motion MR imaging. *Radiology* 1988; 168:497-505
12. Kwon H, Kim HJ, Sol YL, Lee TH, Yeom JA, Kim AR. Usefulness of apparent diffusion coefficient values in the nasopharynx and the oropharynx: differentiation of benign and malignant lesions. *J Korean Soc Radiol* 2012;66:117-122
13. Sasaki M, Eida S, Sumi M, Nakamura T. Apparent diffusion coefficient mapping for sinonasal diseases: differentiation of benign and malignant lesions. *AJNR Am J Neuroradiol* 2011;32:1100-1106
14. Friedrich KM, Matzek W, Gentzsch S, Sulzbacher I, Czerny C, Herneth AM. Diffusion-weighted magnetic resonance imaging of head and neck squamous cell carcinomas. *Eur J Radiol* 2008;68:493-498
15. Habermann CR, Arndt C, Graessner J, Diestel L, Petersen KU, Reitmeier F, et al. Diffusion-weighted echo-planar MR imaging of primary parotid gland tumors: is a prediction of different histologic subtypes possible? *AJNR Am J Neuroradiol* 2009;30:591-596
16. Som PM, Brandwein MS. *Salivary glands: anatomy and pathology.* In Som PM, Curtin HD. *Head and neck imaging, 4th ed*. St. Louis, MO: Mosby, 2003:2005-2133
17. Sumi M, Ichikawa Y, Nakamura T. Diagnostic ability of apparent diffusion coefficients for lymphomas and carcinomas in the pharynx. *Eur Radiol* 2007;17:2631-2637
18. Curtin HD, Ishwaran H, Mancuso AA, Dalley RW, Caudry DJ, McNeil BJ. Comparison of CT and MR imaging in staging of neck metastases. *Radiology* 1998;207:123-130
19. van den Brekel MW. Lymph node metastases: CT and MRI. *Eur J Radiol* 2000;33:230-238
20. Abdel Razek AA, Soliman NY, Elkhamary S, Alsharaway MK, Tawfik A. Role of diffusion-weighted MR imaging in cervical lymphadenopathy. *Eur Radiol* 2006;16:1468-1477
21. Vandecaveye V, De Keyzer F, Vander Poorten V, Dirix P, Verbeken E, Nuyts S, et al. Head and neck squamous cell carcinoma: value of diffusion-weighted MR imaging for nodal staging. *Radiology* 2009;251:134-146
22. de Bondt RB, Hoeberigs MC, Nelemans PJ, Deserno WM, Peutz-Kootstra C, Kremer B, et al. Diagnostic accuracy and additional value of diffusion-weighted imaging for discrimination of malignant cervical lymph nodes in head and neck squamous cell carcinoma. *Neuroradiology* 2009;51: 183-192
23. King AD, Ahuja AT, Yeung DK, Fong DK, Lee YY, Lei KI, et al. Malignant cervical lymphadenopathy: diagnostic accuracy of diffusion-weighted MR imaging. *Radiology* 2007;245: 806-813
24. Koç O, Paksoy Y, Erayman I, Kivrak AS, Arbag H. Role of diffusion weighted MR in the discrimination diagnosis of the cystic and/or necrotic head and neck lesions. *Eur J Radiol* 2007;62:205-213
25. Razek AA, Megahed AS, Denewer A, Motamed A, Tawfik A, Nada N. Role of diffusion-weighted magnetic resonance imaging in differentiation between the viable and necrotic parts of head and neck tumors. *Acta Radiol* 2008;49: 364-370

26. Tartaglino LM, Rao VM, Markiewicz DA. Imaging of radiation changes in the head and neck. *Semin Roentgenol* 1994;29:81-91
27. Terhaard CH, Bongers V, van Rijk PP, Hordijk GJ. F-18-fluoro-deoxy-glucose positron-emission tomography scanning in detection of local recurrence after radiotherapy for laryngeal/ pharyngeal cancer. *Head Neck* 2001;23:933-941
28. Chisin R, Macapinlac HA. The indications of FDG-PET in neck oncology. *Radiol Clin North Am* 2000;38:999-1012
29. Hermans R, Pameijer FA, Mancuso AA, Parsons JT, Mendenhall WM. Laryngeal or hypopharyngeal squamous cell carcinoma: can follow-up CT after definitive radiation therapy be used to detect local failure earlier than clinical examination alone? *Radiology* 2000;214:683-687
30. Lai PH, Yang CF, Pan HB, Wu MT, Chu ST, Ger LP, et al. Recurrent inverted papilloma: diagnosis with pharmacokinetic dynamic gadolinium-enhanced MR imaging. *AJNR Am J Neuroradiol* 1999;20:1445-1451
31. Abdel Razek AA, Kandeel AY, Soliman N, El-shenshawy HM, Kamel Y, Nada N, et al. Role of diffusion-weighted echo-planar MR imaging in differentiation of residual or recurrent head and neck tumors and posttreatment changes. *AJNR Am J Neuroradiol* 2007;28:1146-1152
32. Baur A, Huber A, Arbogast S, Dürr HR, Zysk S, Wendtner C, et al. Diffusion-weighted imaging of tumor recurrencies and posttherapeutical soft-tissue changes in humans. *Eur Radiol* 2001;11:828-833
33. Maier CF, Paran Y, Bendel P, Rutt BK, Degani H. Quantitative diffusion imaging in implanted human breast tumors. *Magn Reson Med* 1997;37:576-581
34. Eis M, Els T, Hoehn-Berlage M. High resolution quantitative relaxation and diffusion MRI of three different experimental brain tumors in rat. *Magn Reson Med* 1995;34:835-844
35. Chenevert TL, McKeever PE, Ross BD. Monitoring early response of experimental brain tumors to therapy using diffusion magnetic resonance imaging. *Clin Cancer Res* 1997;3:1457-1466
36. Poptani H, Puumalainen AM, Gröhn OH, Loimas S, Kainulainen R, Ylä-Herttuala S, et al. Monitoring thymidine kinase and ganciclovir-induced changes in rat malignant glioma in vivo by nuclear magnetic resonance imaging. *Cancer Gene Ther* 1998;5:101-109
37. Tsuruda JS, Chew WM, Moseley ME, Norman D. Diffusion-weighted MR imaging of the brain: value of differentiating between extraaxial cysts and epidermoid tumors. *AJR Am J Roentgenol* 1990;155:1059-1065; discussion 1066-1068
38. Brunberg JA, Chenevert TL, McKeever PE, Ross DA, Junck LR, Muraszko KM, et al. In vivo MR determination of water diffusion coefficients and diffusion anisotropy: correlation with structural alteration in gliomas of the cerebral hemispheres. *AJNR Am J Neuroradiol* 1995;16:361-371
39. Chenevert TL, Stegman LD, Taylor JM, Robertson PL, Greenberg HS, Rehemtulla A, et al. Diffusion magnetic resonance imaging: an early surrogate marker of therapeutic efficacy in brain tumors. *J Natl Cancer Inst* 2000;92:2029-2036
40. Mardor Y, Pfeffer R, Spiegelmann R, Roth Y, Maier SE, Nissim O, et al. Early detection of response to radiation therapy in patients with brain malignancies using conventional and high b-value diffusion-weighted magnetic resonance imaging. *J Clin Oncol* 2003;21:1094-1100
41. Zhao M, Pipe JG, Bonnett J, Evelhoch JL. Early detection of treatment response by diffusion-weighted 1H-NMR spectroscopy in a murine tumour in vivo. *Br J Cancer* 1996;73:61-64
42. Stegman LD, Rehemtulla A, Hamstra DA, Rice DJ, Jonas SJ, Stout KL, et al. Diffusion MRI detects early events in the response of a glioma model to the yeast cytosine deaminase gene therapy strategy. *Gene Ther* 2000;7:1005-1010
43. Moffat BA, Chenevert TL, Lawrence TS, Meyer CR, Johnson TD, Dong Q, et al. Functional diffusion map: a noninvasive MRI biomarker for early stratification of clinical brain tumor response. *Proc Natl Acad Sci U S A* 2005;102:5524-5529
44. Lee KC, Moffat BA, Schott AF, Layman R, Ellingworth S, Juliar R, et al. Prospective early response imaging biomarker for neoadjuvant breast cancer chemotherapy. *Clin Cancer Res* 2007;13(2 Pt 1):443-450
45. McVeigh PZ, Syed AM, Milosevic M, Fyles A, Haider MA. Diffusion-weighted MRI in cervical cancer. *Eur Radiol* 2008;18:1058-1064
46. Kim S, Loevner L, Quon H, Sherman E, Weinstein G, Kilger A, et al. Diffusion-weighted magnetic resonance imaging for predicting and detecting early response to chemoradiation therapy of squamous cell carcinomas of the head

and neck. *Clin Cancer Res* 2009;15:986-994
47. Chinnaiyan AM, Prasad U, Shankar S, Hamstra DA, Shanaiah M, Chenevert TL, et al. Combined effect of tumor necrosis factor-related apoptosis-inducing ligand and ionizing radiation in breast cancer therapy. *Proc Natl Acad Sci U S A* 2000;97:1754-1759
48. Kauppinen RA. Monitoring cytotoxic tumour treatment response by diffusion magnetic resonance imaging and proton spectroscopy. *NMR Biomed* 2002;15:6-17
49. Cao Y, Popovtzer A, Li D, Chepeha DB, Moyer JS, Prince ME, et al. Early prediction of outcome in advanced head-and-neck cancer based on tumor blood volume alterations during therapy: a prospective study. *Int J Radiat Oncol Biol Phys* 2008;72:1287-1290
50. Schmitt P, Kotas M, Tobermann A, Haase A, Flentje M. Quantitative tissue perfusion measurements in head and neck carcinoma patients before and during radiation therapy with a non-invasive MR imaging spin-labeling technique. *Radiother Oncol* 2003;67:27-34
51. Robinson SP, Collingridge DR, Howe FA, Rodrigues LM, Chaplin DJ, Griffiths JR. Tumour response to hypercapnia and hyperoxia monitored by FLOOD magnetic resonance imaging. *NMR Biomed* 1999;12:98-106
52. Zima A, Carlos R, Gandhi D, Case I, Teknos T, Mukherji SK. Can pretreatment CT perfusion predict response of advanced squamous cell carcinoma of the upper aerodigestive tract treated with induction chemotherapy? *AJNR Am J Neuroradiol* 2007;28:328-334
53. Pruessmann KP, Weiger M, Scheidegger MB, Boesiger P. SENSE: sensitivity encoding for fast MRI. *Magn Reson Med* 1999;42:952-962
54. Willinek WA, Gieseke J, von Falkenhausen M, Neuen B, Schild HH, Kuhl CK. Sensitivity encoding for fast MR imaging of the brain in patients with stroke. *Radiology* 2003;228:669-675
55. Yoshino N, Yamada I, Ohbayashi N, Honda E, Ida M, Kurabayashi T, et al. Salivary glands and lesions: evaluation of apparent diffusion coefficients with split-echo diffusion-weighted MR imaging--initial results. *Radiology* 2001;221:837-842
56. Kito S, Morimoto Y, Tanaka T, Tominaga K, Habu M, Kurokawa H, et al. Utility of diffusion-weighted images using fast asymmetric spin-echo sequences for detection of abscess formation in the head and neck region. *Oral Surg Oral Med Oral Pathol Oral Radiol Endod* 2006;101:231-238
57. Grieve SM, Blamire AM, Styles P. Elimination of Nyquist ghosting caused by read-out to phase-encode gradient cross-terms in EPI. *Magn Reson Med* 2002;47:337-343
58. Vandecaveye V, De Keyzer F, Nuyts S, Deraedt K, Dirix P, Hamaekers P, et al. Detection of head and neck squamous cell carcinoma with diffusion weighted MRI after (chemo) radiotherapy: correlation between radiologic and histopathologic findings. *Int J Radiat Oncol Biol Phys* 2007;67:960-971

두경부 종양의 평가에 있어서 확산강조영상의 역할과 유용성: 종설[1]

설유리[1] · 김학진[1] · 이병주[2]

두경부 악성종양의 영상검사로 MRI와 CT가 가장 적절하다. 그러나 이 둘은 두경부 종양의 진단, 병기결정 및 치료 후 평가 등에 있어서 민감도와 정확도가 떨어진다. 이 종설은 두경부 종양에서 확산강조영상의 역할과 유용성에 대해 살펴본다. 확산강조영상은 조직을 현미경적 수준으로 분석하는 기법이며 여기서 나온 apparent diffusion coefficient 값은 종양과 비종양조직의 미세구조 차이를 구분할 수 있다. 따라서 확산강조영상은 두경부 종양의 병리조직 특성, 감별진단, 병기결정 및 치료 후 평가 등에 도움이 되는 정보를 제공하여 임상적으로 유용한 기법이다.

부산대학교 의과대학 부산대학교병원 의생명연구원 [1]영상의학과, [2]이비인후과